Immunoglobulin G ions as-electrosprayed are slightly less compact in dry than in humid air

Juan Fernandez de la Mora,[a] Rian You[b,c] and Michael R. Zachariah[b,c]

[a] Yale University, Department of Mechanical Engineering and Materials Science

[b] University of Maryland, College Park, Maryland 20742

[c] National Institute of Standards and Technology, Gaithersburg, Maryland 20899.

First submitted to Analytical Chemistry (20/Aug/2015); revised 1/March/2016

Second revision and first submission to J. Phys. Chem. B: 8/March/2017

ABSTRACT

Dialysis purification of immunoglobulin G (IgG) followed by electrospraying in an aqueous solution with 100 mM triethylammonium formate results in protein ion peaks sufficiently narrow (relative full width at half maximum FWHM=3-4%) to accurately define their electrical mobility immediately after ionization, under ambient conditions of temperature and pressure. The protein cross section measured in dry air is found to be only 3% larger than in air nearly saturated with water vapor, implying that the just formed dry ion is almost as compact as the solvated and perhaps still native structure. This finding contributes partial confirmation to the proposal of Breuker and McLafferty that dry protein ions exhibiting minimal (surface) structural variations over the solution structure are stable in the gas phase within ms times. If this were true, their solution collision cross section could be measured in the gas phase with suitably soft and fast methods, such as those used here (a differential mobility analyzer responding in ≈100 μs). Paradoxically, the protein has a cross section 3% smaller when solvated than when dry, revealing a small but measurable structural shift associated with drying.

1. INTRODUCTION

Numerous studies of gas phase proteins by ion mobility spectrometry (IMS) and mass spectrometry (MS) of their electrosprayed ions have been published in recent years.[1,2,3] These investigations are often aimed at inferring the structure of the gas phase ion, which under favorable conditions is believed to be closely related to the solution structure prior to spraying. However, the initial ion structure immediately after electrospraying is apparently transient [4] and not easily probed. In the picture drawn by Breuker and McLafferty,[4] some protein surface rearrangement takes place immediately after complete drying, with charged groups burying themselves within the bulk, presumably resulting in a reduced cross section. These proposed initial dry structures would be of considerable interest, as they would preserve essentially all the solution conformation except for the minor surface rearrangements noted. These early dry conformations are apparently stable only within ms time scales, being difficult to maintain prior to mobility measurement because of various excitations arising in real life instruments (vigorous heating at the ion source, energetic collisions at the vacuum interface and the ion guides, excitation on injecting the ions into a drift cell, or upon maintaining lateral confinement. Also, typical ion mobility measurement drift times are tens of ms.

A few reports of sub ms ambient pressure mobility measurements prior to MS identification have suggested that differences between ambient and low pressure mobilities arise.[5] However, ambient mobility measurements have not yet captured the hypothetical Breuker-McLafferty dry transient structures, nor compared them with low pressure measurements.

One significant barrier to ambient cross section studies of native proteins electrosprayed from neutral aqueous solutions is that they form ions via Dole's charged residue mechanism.[6]

They hence attach to involatile impurities in the solution drops, which widens their mass and mobility distribution. At reduced pressure, this problem is alleviated via de-clustering ion-gas collisions, but this method implies a risk of changing the protein structure, and is unpractical at atmospheric pressure. As a general rule, the larger a protein, the harder it is to achieve a clean mobility spectrum, a point clearly seen in prior studies with immunoglobulins.[7,8,9,10,11,12,13] The clustering problem may be moderated by solution cleaning, and by minimizing the initial volume of electrospray drops (nanospray). Both approaches are implemented here for immunoglobulin G (IgG; molecular weight ≈150,000 Da), resulting in singularly narrow mobility peaks whose cross sections can be precisely determined. This enables measurements in air sufficiently precise to show that an environment nearly saturated with water vapor reduces some 3% the protein cross section. This finding apparently implies that the solvated and presumably still native structure differs very little from the just formed completely dry structure, in qualitative agreement with the Breuker-McLafferty view.[4] Unexpectedly, the dry structure is slightly less mobile rather than slightly more mobile than the solvated ion.

2. EXPERIMENTAL

Mobility measurement: Mobility spectra were determined in a previously described parallel-plate differential mobility analyzer (DMA)[14], based on a SEADM design.[15] The instrument operates in the linear mobility regime, where the product of the DMA voltage at which an ion is selected times its electrical mobility $V_{DMA}Z$ is a constant for all ions, whose value is determined by calibration with the tetrahexadecylammoniom$^+$ ion (C_{16}^+).[16] The distance between DMA plates is 1 cm, and the streamwise distance between slits is 2 cm. The ES

chamber is similar to that of [15], where the electrospraying needle can be brought arbitrarily close to the inlet slit of the DMA. The resolving power with 1 nm clusters exceeds 50 at the sample flow rates q_s<3 lit/min used in this work. The sheath gas flow runs in closed circuit, driven by a blower followed by a HEPA filter. An input of humidity-controlled flow of bottled air (q_i≈2.8 lit/min) is introduced on the closed circuit right upstream of the blower. Part of it (q_o≈2.8 lit/min) is sampled at the outlet slit of the DMA carrying mobility-selected ions. The associated ion current is detected in a Faraday cage electrometer. In a few experiments the detector was a condensation particle counter (CPC; TSI model 3760), in which supersaturated butanol vapor condenses on the IgG ions, growing them into micron size drops that are individually detected optically. In CPC studies the sample flow rate q_o was fixed at 1.5 lit/min. The small balance $q_{CF}=q_i-q_o$ (≈0.1 lit/min) of input flow not drawn into the detector moves through the inlet slit from the DMA into the ES chamber as a counterflow gas, designed to avoid entry of vapors from the ES chamber into the DMA. As a result, the gas circulating in closed loop through the DMA has the composition of the input gas injected into the closed circuit at flow rate q_i. The ions produced in the ES chamber penetrate through the inlet slit, driven by electric fields against the exiting counterflow gas. The mobilities reported are corrected to standard atmospheric pressure. The DMA pressure relative to the lab (a few tens of mb) was measured with a digital manometer [Fisher Scientific™ Traceable™ Manometer]. The absolute ambient pressure was read (hourly) from the web page at New Haven's Tweed airport.

Humidity control: The input gas flow rate q_i, controlled with a rotameter, went through a *saturator* bottle (0.5 lit internal volume) before entering the closed circuit of the DMA. The

humidity was controlled by introducing the *saturator* bottle in a temperature controlled bath (either refrigerant liquid at -3 ^{o}C or a water bath at 20 ^{o}C), or by removing the saturator bottle from the inlet gas circuit (*dry* condition). The recirculating gas was slightly heated by the blower (25^{o}C at the DMA inlet vs. ≈20^{o}C ambient), precluding vapor condensation.

Materials: 10 mg of IgG (Sigma Aldrich; # I4506, Lyophilized powder from human plasma) were dissolved in 0.2 ml of deionized water containing 2 mM ammonium acetate (pH=7.4). The resulting 341 μM solution of IgG was equally divided into two shares and pipetted into two minidialysis devices (ThermoScientific 10 K MWCO, Slide-A-Lyzer MINI Dialysis Devices, 0.1 ml) that were inserted in vials containing 2 mM ammonium acetate. The assemblies were then vortexed for 30 minutes, following which the 2 mM ammonium acetate in the vials was replaced with a fresh one, and vortexing was continued for another 30 minutes. The sample dialyzed at NIST was shipped to the Yale lab (in a frozen package) at a protein concentration of about 300 μM in 2 mM ammonium acetate, and was subsequently stored in a refrigerator. Prior to mobility analysis the NIST protein sample was diluted 100 fold in a buffer of deionized water including 100 mM triethylammonium formate (TEAF; from a 1 M aqueous solution from Fluka). Accordingly, the electosprayed liquid was in all cases aqueous 100 mM TEAF with 3μM IgG and 0.2 mM ammonium acetate. The TEAF buffer was selected over an ammonium acetate buffer because it yields lower charge states that are more easily separated by mobility alone.

The emitting ES needle was a commercial silica capillary (360 μm OD; 170μm ID; Polymicro Technologies) home-drawn under a flame down to a ≈20 μm tip. It formed stable Taylor cones with no signs of electrical discharges, typically emitting 300 nA of ES current.

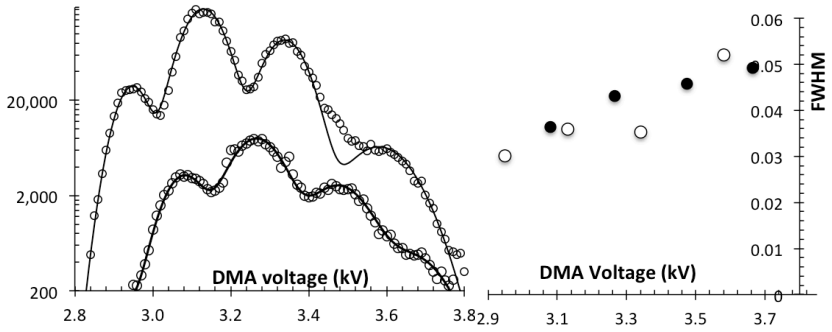

Figure 1: Left: mobility spectra of IgG in dry air, displaying several mobility peaks corresponding to various charge states. The Gaussian fittings reveal the FWHM values represented on the right figure, approaching 3% for the most mobile peaks.

3. RESULTS

The viability of achieving narrow IgG mobility peaks is demonstrated in Figure 1 through two representative raw mobility spectra (left) obtained under different operating conditions. The right figure represents the relative full width at half maximum (FWHM) of these various peaks, inferred from the Gaussian fits shown, revealing values approaching 3% in the most mobile peaks. This width is several times smaller than previously observed for this large protein, attesting either to the success of the cleanup process, or to the advantage of probing the ions fast (<1ms) under thermal conditions. We find a systematic increase in peak width with decreasing charge state, to be later discussed.

Charge assignment, ion identification and measured cross section

Details on peak assignment and Tables of their mobilities are given in auxiliary information (in the web). Briefly, the ions were charge-reduced with the help of a Ni-63 source of beta particles,[17] producing the mobility spectra in dry air shown in Figure 2. The least mobile ion in the series (not shown) is assigned z=1, and the subsequent members are serially assigned

values 2, 3, … 18, as labelled in the Figure. This serial assignment is confirmed by the approximate proportionality between z and the mobility Z, which is almost exact for the lower charge states. Figure 2 shows also several weaker peaks, part of a different sequence of less mobile ions associated to the dimer of IgG (peaks between z=2 and 3 and between z=4 and 5), whose relatively low abundance provides further assurance that the dominant series of ions is indeed associated to the IgG monomer. Given the relatively low electrical mobility of charge-reduced ions, this work was done with a different DMA having a cylindrical geometry.[18]

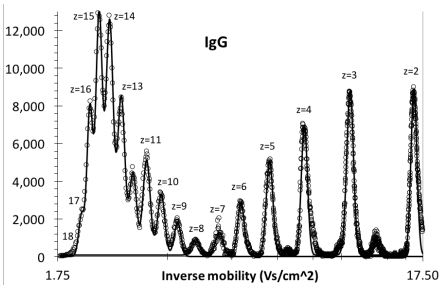

Figure 2: Charge-reduced mobility spectrum of IgG in dry air enabling determination of the charge state. The absolute mobility scale reported is based on the C16 standard. T=23^{o}C.

Interestingly, the peak widths in Figure 2 span the range of relative FWHM from 4.1% to 5.5%, with additional non-Gaussian low mobility tails (right tails in Figure 2), particularly clear in the low-z peaks. We attribute these differences with the measurements in Figure 1 to the longer time scales involved with the use of the cylindrical DMA and the charge reduction process.

Charge state dependence on flight distance. Upon reducing the distance L from the emitting tip to the sampling slit of the DMA, in addition to a rising signal, the charge state increases (Figure 3 left), as previously reported.[19] This cannot be due to space charge dilution of high-mobilities, since all ions follow approximately the same electric field lines. We attribute the preferential loss of high z ions at large distances to the often observed fact that highly charged proteins are unstable and tend to shed one or several charging species at a certain ion evaporation rate. As L increases, so does the flight time and the net charge loss. This mechanism is documented in the supplementary information via tandem DMA experiments with ovalbumin. A charge state z selected in DMA_1 appears in DMA_2 as z, z-*1*, z-*2*, … , without any activation in between and in ≈10 ms time scales, with complete loss in some cases of the parent ion. Similarly facile charge losses have been reported in DMA-MS experiments both with polymers[20] and proteins,[21] though in these cases ion evaporation might have been activated at the MS inlet.

The observed charge evaporation also hints at an explanation for why the highest charge states seen have narrower mobility peaks: Unstable ions having lost one or more charges just before entering the DMA might not have yet achieved the steady conformation corresponding to their new charge state, presenting a range of conformations.

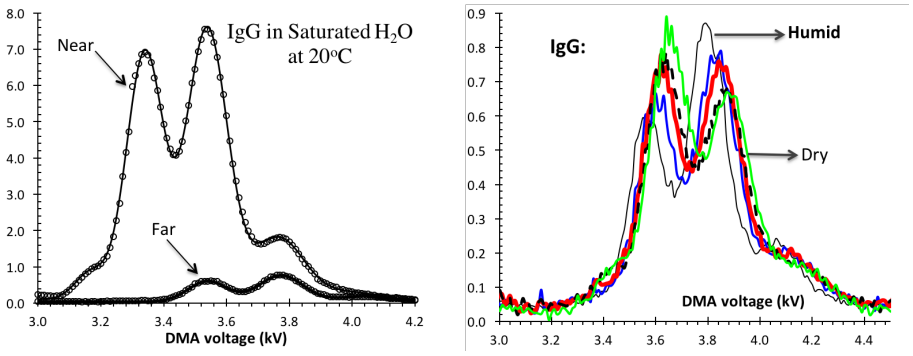

Figure 3: Mobility spectra for IgG in air: Left, loss of higher charge states on increasing the ES to DMA distance *L*. Right: Effect of drying the carrier gas in decreasing protein mobility

Effect of humidity. Figure 3 (right) shows the evolution of the mobility spectra of IgG as the humidity level slowly decays in time; from an initial nearly saturated state with the saturator held first at 20 ^{o}C (p_{H2O}≈23 mb, labelled *Humid*); then at -3 ^{o}C (p_{H2O}≈4.7 mb), and finally into the completely dry situation resulting from removing the saturator from the input gas circuit (p_{H2O}≈0 mb, labelled *Dry*). No pressure corrections on mobility calibration are needed after removal of the saturator from the circuit, as the DMA pressure (1041 mb) and temperature (25 ^{o}C) changed less than 1 mb and 1 ^{o}C, respectively through the whole series of measurements. The intermediate sequence of temperatures cannot be quantitatively associated to a sequence of precise humidities because the response time of the system to a change in humidity is on the range of 10 minutes. The initial and final humidities do however correspond quantitatively to the initial (leftmost) and final (rightmost) mobility spectra, since the circuit was kept over these two (initial and final) fixed states for a long enough time for the positions of the peaks to converge to a steady value. The qualitative information obtained at intermediate humidities shows that the peak width and the mobility evolve monotonically through a narrow range of mobilities over the full 0-100% water vapor content range.

Peak voltages for 100% and 0% humidity are collected in Table 1. Except for the datum at the smallest *z* (whose weak intensity precludes an accurate voltage measurement), drying leads to a 3.5% voltage increase. The charge states in the Table are inferred (without direct calibration) by comparing the series of dry ion voltages with those for Figure 2 (details in the web portion of the article).

Table 1: Peak voltages V, and tentative charge assignments z for IgG ions under dry and humid conditions

z	18	17	16	15	14
V(kV) sat @ 20 ^{o}C	3.158	3.330	3.528	3.755	4.030
V(kV) Dry		3.450	3.650	3.883	4.143
V(dry)/V(humid)		1.036	1.035	1.034	1.028

The conversion of a DMA voltage V_{DMA} into an ion mobility Z, and the inference of a protein cross section $\Omega \approx z/Z$ from this Z value require attention. Under saturation at 20 ^{o}C, the molar fraction of water would be 23/1041=2.21%, calling for composition corrections in deriving a cross section from the mobility shift observed. Two composition corrections are relevant. (i) One associated to the fraction of collisions of the protein ions with water molecules. (ii) The other due to humidity corrections in the DMA calibration constant.

(i) The drag coefficient of the protein moving in a mixed bath gas is the sum of the drags associated to each of the gases, each of which is proportional to the partial pressure of the gas divided by its thermal speed times the cross sectional area of the target ion presented to the bath. Ignoring long range interactions, because water molecules are lighter than air molecules the drag decreases, making the relative change in cross section smaller than the 3.5% relative voltage change observed. In the case of a spherical ion, the cross section would be proportional to the square of the sum of the ion diameter d and the effective diameter δ of the bath gas molecule:

$$1/Z_i = \beta p_i (d+\delta_i)^2 m_i^{1/2}, \qquad (1)$$

where β is the same proportionality constant for the two gases, the subscript i stands for either air or water vapor, and we use the fact that the thermal speed is proportional to the -½ power of the effective mass (which for our massive proteins is indistinguishable from the mass m_i of either bath gas). Accordingly, the addition rule for the drag yields

$$1/Z=\beta p[x_{air}(d+\delta_{air})^2 m_{air}^{1/2}+ x_{H2O}(d+\delta_{H2O})^2 m_{H2O}^{1/2}], \qquad (2)$$

where $x_i=p_i/p$; $p=p_{air}+p_{H2O}$. Using Z_o for the ion mobility in dry air and x for x_{H2O} we find

$$Z_o/Z=1+x[-1+(18/28.97)^{1/2}(d+\delta_{H2O})^2/(d+\delta_{air})^2]. \qquad (3)$$

Given the large disparity in protein versus gas diameters (d=9 nm [22] and δ_{air} =0.25 nm in room temperature air[23]), $(d+\delta_{H2O})^2/(d+\delta_{air})^2 \approx 1+2(\delta_{H2O}-\delta_{air})/d = 1+2[\delta_{air}/d][(\delta_{H2O}-\delta_{air})/\delta_{air})]$ $=1+0.055(\delta_{H2O}-\delta_{air})/\delta_{air}$. Since $(\delta_{H2O}-\delta_{air})/\delta_{air}$ should itself be small, $1+2(\delta_{H2O}-\delta_{air})/d$ may differ from unity by a few percent at most. Therefore, to an excellent approximation

$$Z_o/Z=1-0.21x_{H2O}, \qquad (4)$$

which differs from unity at most by 0.46%. Even though IgG is non-spherical, the simplification that its cross sections in air and water vapor are very close to each other still applies for any large ion, justifying more generally the result (4). Therefore, this correction would make the reduction in cross section associated to humidification to be 3.5%-0.46% ≈3%. We have so far ignored long range interactions due to a permanent and an induced dipole between the ion and the water molecules. The permanent dipole effects are difficult to quantify, as there is no agreement between measurements and theory.[24] However, they are undoubtedly stronger for water than air molecules, so, correcting for them would make the relative change in cross section larger than 3%.

(ii) The effect of humidity on the DMA calibration constant $V_{DMA}Z$ is a second concern. We would need an ion standard of known mobility under dry and saturated conditions. Even for

highly hydrophobic substances like tetrahexadecylammonium$^+$ it would be unsafe to assume that no hydration at all would take place. Accordingly, we have inferred the humidity shift of *ZV* based on the expected response of the blower. *ZV* is proportional to the volumetric flow rate *Q* of gas through a strictly geometrical constant $k=ZV/Q$. The blower is operated at constant speed of rotation ω, pressure and temperature. The compression ratio is rather modest, making compressibility almost irrelevant. Viscous effects at the prevailing high Reynolds numbers will not shift noticeably by a slight change in Reynolds number. Therefore, the pressure increase in the compressor made dimensionless with the dynamic pressure $\rho Q^2/R^4$ depends only on the ratio of rotation to flow speeds:

$$\Delta p R^4/(\rho Q^2)=F(\omega R^3/Q), \qquad (5)$$

where ρ is the gas density and *R* is a characteristic length of the blower. Also, this pressure increase is equal to the pressure drop in the closed DMA circuit, which is itself linear in the dynamic pressure $\rho Q^2/R'^4$, where R'^2 is the throat area of either the DMA channel or a smaller constriction placed in the closed circuit. Consequently, the ρQ^2 terms in the numerator and denominator of the left hand side of Equation (5) cancel, making the left hand side constant: $\omega R^3/Q$ =constant. *Q* is then linear with ω, with no composition dependence:

$$Q \sim \omega, \qquad (6)$$

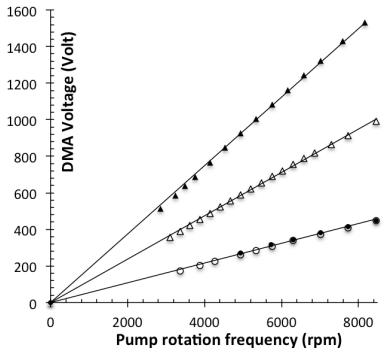

Figure 4: Blower response given as mean peak voltage versus rotation frequency $V_{DMA}(\omega)$ obtained for three different flow restrictions inserted in the closed circuit. Because $Q \sim V_{DMA}$, the data validate Equation (6) at ω>4000 rpm.

The validity of Equation (6) is tested in Figure 4, which plots the mean voltage for the (unidentified) dominant peak obtained when electrospraying pure water as a function of the rotation frequency. The three curves displayed were obtained in dry air for three different positions of a ball valve inserted into the circuit so as to modify the flow resistance. Since the DMA voltage associated to a given ion is strictly proportional to the flow rate Q through the closed circuit, Equation (6) would require that the data in Figure 4 be on a straight line going through the origin of coordinates. This prediction is well satisfied at rotation frequencies higher than about 4000 rpm. All three curves bend slightly downwards at lower ω, probably because the Reynolds number in the pump ceases to be large enough for viscous effects to have a negligible influence. In conclusion, we expect no direct dependence of the calibration constant on the humidity level: only secondary dependences associated to slight viscous and compressibility effects. These weak secondary humidity effects combined with the small relative variation in density and viscosity following humidification result in negligible changes in calibration constant. Indeed, similarly as in Equation (4), we may write

$$\rho/\rho_o = 1 + x_{H2O}[-1 + m_{H2O}/m_{air}] = 1 - 0.37\, x_{H2O}. \qquad (7)$$

No careful quantitative replicate measurements were made, but multiple dry mobility measurements were taken. Some are included in the web section, noting run to run variations of 0.5%. The observed 3.5% voltage shift on humidifying, being relative, is even more repeatable. The main ambiguity on our quantification of the 3% effect of humidity on cross

section is associated to the calibration constant ZV, through the hypothesis (6) that $Q \sim \omega$, with no humidity dependence. Examination of Figure 4 shows that errors in a strict $Q \sim \omega$ dependence are surely less than 5%, so that the calibration error would be at most 5% of the density change, which according to Equation (7) does not exceed 1%. The net calibration error would then be less than $5\ 10^{-4}$.

In conclusion, by correcting approximately the 3.5% voltage reduction seen upon humidification, we find that humidification reduces the protein cross section by at least 3%. This is most unusual. All other (small) ions in our spectra decrease their mobility in a humid environment, as would be expected as a result of solvation.[25] Similarly, a recent study adding up to 1.5-2% (vol) of other vapors (ammonia, hexane, methanol, formic acid, isopropanol and tert-pentanol) found that all but ammonia and hexane increased substantially (and nonlinearly with vapor concentration) the cross section of cytochrome c. Addition of 1.5 % ammonia or hexane increased the cross section also, but linearly with vapor concentration, and only by ≈ 2 % and ≈5%, respectively.[26] Interestingly, the linear cross section increase for hexane showed that the ratio of apparent protein cross sections in pure air and pure hexane is almost four times larger than unity, which in light of the analysis leading to our Equation (4) suggests that also heptane vapors are affecting the conformation. This anomalous linear response found may imply that heptane and ammonia disrupt the protein structure in a transient and reversible manner, rather than catastrophically as most other vapors. In any case, these results leave no doubt about the high sensitivity of protein structure to solvation by various vapors. It is therefore unsurprising that water vapor would not only also affect the gas phase structure of the protein, but (given the special relation between proteins and water) that the direction of this effect in water would be the opposite as that in most other gases.

Discussion. Proteins crystals are hydrophilic, and cannot be dried until the ambient is well below saturation. However, a neutral object 9 nm in diameter in a saturated atmosphere would ordinarily be completely dry because the Kelvin effect increases drastically the vapor pressure over a surface of high curvature. On the other hand, a small ion in a nearly saturated vapor would be substantially solvated because solvation reduces its large electrostatic energy. While deliquescence of hydrophilic particles considerably larger than 9 nm is often observed below saturation, this has never been observed on any protein. Furthermore, when passed through the highly supersaturated (in butanol) atmosphere of our CPC detector, only a modest fraction of IgG monomers do grow to visible sizes, as evident from the disproportionately large dimer/monomer signal observed with the CPC versus an electrometer. We therefore expect an *almost dry* protein even under 100% humidity, with local solvation only at its charged groups. In the picture of Breuker and McLafferty the initially solvated protein first moves into this *almost dry* state (only the charged groups are solvated) with no structural shifts, and then dries completely, with minor structural shifts. Our own proteins do likewise, except that they may switch between these two states as their environment switches from humid to dry. Several possible interpretations of this strong analogy suggest themselves.

(A) Our observation that the ion mobility shifts only 3% from one state to the other agrees qualitatively with the Breuker-McLafferty prediction that there is very little structural shift following complete protein ion drying, at least within sub millisecond times. This coincidence seems at first sight to provide support for the commonly held (yet sometimes contested[21]) notion that structures almost identical to the native solution structures may

be probed by ion mobility studies in the gas phase. The considerable importance of this possibility (in principle) has been widely appreciated in this field. In practice, however, there is no assurance that the ions probed in the two phases will be identical, unless they are probed fast and are subject to minimal disruptions following desolvation. These requirements are unfrequently met in IMS-MS work as rigorously as here. On the other hand, the observation of a minimal change in conformation following complete drying is also expected in the hypothesis that the protein rapidly adopts a gas phase conformation quite different from the solution structure. The reason is that an important driving force for structural changes on moving into the gas phase is the capillary stress tending to spheroidize a moderately deformable ion. This capillary compression is initially due to the surface tension of the water drop; but it remains active after complete drying of the liquid because the effective surface tension of protein matter is comparable to that of water.[21] Therefore, our measurements do not by themselves support the notion that the partly solvated gas phase ion retains its prior solution structure. This notion must rest elsewhere. What our measurements confirm is that the completely dried ion is structurally quite close to the slightly solvated ion. Similar conclusions have been reached in experiments *solvating* several charged sites of cytochrome C with crown ethers (18-crown-6, 264 Da).[27] The native-like structure seen at z=5 had a cross section only minimally increased by this *solvation*. Perhaps Cytochrome C would have also displayed the slightly reduced cross section found here if corrections had been made for the added surface associated to the attached crown ethers (these corrections would however be more challenging than those implemented here). For z≥7 the cross section of the *solvated* protein was smaller than the *unsolvated* one, but larger than the native-like

structure forming at z=5. This observed increased stability against Coulombic stresses was attributed to inhibition by the *solvating* crowns of a destabilizing tendency for the charged side chains to collapse onto the protein backbone. Although this stabilizing mechanism was invoked in relation to Coulombically stretched conformations, perhaps it would apply also to the native-like structures seen at low *z*, contributing to rationalize the slight compaction effects we observe here.

(B) We finally consider the sign of the tiny change observed here following complete drying, which is, paradoxically, a slightly *increased* cross section. In the Breuker-McLafferty picture, the initially solvated ions stick out of the protein, and bury themselves within the protein bulk after complete drying, so the cross section *decreases* on drying. The same slight *decrease* would be expected for a gas phase structure different from the solution conformation, if, upon drying, it would simply lose a few surface water molecules without additional structural changes. It therefore follows from our measurements that complete drying leads to a slight but noticeable change in the protein structure that makes it appear as less compact. This slight shift is not incompatible with the Breuker-McLafferty key point that the tertiary structure is initially preserved by complete drying (the shift is small, and our charges are adducted triethylammonium ions rather than the protons considered in the simulations). Alternatively, those believing that the gas phase protein tends to be compacted by capillary stresses could conveniently argue that an effective surface tension of protein matter slightly smaller than that of water is not incompatible with known facts.

CONCLUSIONS

Exceptionally narrow mobility peaks have been obtained for IgG at ambient temperature and pressure, without declustering, heating, or other collisional activations that could affect its original conformation as electrosprayed. These singularly narrow peaks for such a large protein have resulted from improved solution cleaning, as well as the use of a parallel plate DMA measuring mobility within submiliseconds of ion formation. The narrowest peaks observed (relative FWHM of 3%) correspond to the highest charge states *z*, which quickly evolve by ion evaporation towards lower *z,* without any external activation. Peak widening observed at decreasing *z* or in measurements taking tens of ms with a different DMA is likely due to natural ion structure evolution with time, with development of low mobility tails without appreciably shifting the position of the peak maximum.

The well defined peaks obtained have enabled accurate measurements on the effect of humidity on IgG structure. As expected, drying varies the structure very little. Unexpectedly, a measurable 3% cross section decrease arises on going from 0% to 100% humidity.

Supporting Information is included on (S1) Tandem DMA studies of spontaneous ion evaporation from protein ions; (S2) Assignment of charge states and IgG ion identification; (S3) Protein cross section

Conflict of interest: Following Yale rules, Juan Fernandez de la Mora declares that he has a personal interest in the company SEADM commercializing the parallel plate differential mobility analyzer used in this research.

Disclaimer: Certain commercial equipment, instrument or materials are identified in this

paper to foster understanding. Such identification does not imply recommendation or endorsement by the National Institute of Standards and Technology, nor does it imply that the materials or equipment identified are necessarily the best available for the purpose.

Acknowledgment: Partial support was received from NanoEngineering Corporation, and DARPA Grant W31P4Q13C0073 (Connecticut Analytical Corporation subcontract).

REFERENCES

[1] D.E. Clemmer, M.F. Jarrold, Ion mobility measurements and their applications to clusters and biomolecules, J. Mass Spectrom., 32, 577-592, 1997

[2] B. C. Bohrer, S. I. Merenbloom, S. L. Koeniger, A. E. Hilderbrand, D. E. Clemmer, Biomolecule Analysis by Ion Mobility Spectrometry, Ann. Rev. Anal. Chem., 1: 293-327, 2008

[3] B. T. Ruotolo, J. L. P. Benesch, A. M Sandercock, S.J. Hyung, C. V Robinson, Ion mobility–mass spectrometry analysis of large protein complexes, Nature Protocols 3, 1139-1152, 2008

[4] K. Breuker and F. W. McLafferty, Stepwise evolution of protein native structure with electrospray into the gas phase, Proc. Natl. Acad. Sci. U. S. A., 2008, 105, 18145-18152.

[5] Hogan, C.; Ruotolo, B.; Robinson, C.; Fernandez de la Mora, J.. Tandem Differential Mobility Analysis-Mass Spectrometry Reveals Partial Gas-Phase Collapse of the GroEL Complex, J. Phys. Chem. B, 115**(**13), 3614-3621**,** 2011

[6] Fernandez de la Mora, J., Electrospray ionization of large multiply charged species proceeds via Dole's charged residue mechanism, Anal. Chim. Acta, **406**, 93-104, 2000.

[7] C. N. Ferguson, S. A. Benchaar, Z. Miao, J. A. Loo, H. Chen, Direct Ionization of Large Proteins and Protein Complexes by Desorption Electrospray Ionization-Mass Spectrometry, Anal. Chem. 2011, 83, 6468–6473

[8] D. Bagal, J. F. Valliere-Douglass, A. Balland, P. D. Schnier, Resolving Disulfide Structural Isoforms of IgG2 Monoclonal Antibodies by Ion Mobility Mass Spectrometry, Anal. Chem. 2010, 82, 6751–6755

[9] C. W. N. Damen, W. Chen, A. B. Chakraborty, M. van Oosterhout, J. R. Mazzeo, J. C. Gebler, J. H. M. Schellens, H. Rosing, J. H. Beijnen' Electrospray Ionization Quadrupole Ion-Mobility Time-of-Flight Mass Spectrometry as a Tool to Distinguish the Lot-to-Lot Heterogeneity in N-Glycosylation Profile of the Therapeutic Monoclonal Antibody Trastuzumab (IgG1), J Am Soc Mass Spectrom 2009, 20, 2021–2033

[10] F. Debaene, E. Wagner-Rousset, O. Colas, D. Ayoub, N. Corvaïa, A. VanDorsselaer, A. Beck, S. Cianfeŕani, Time Resolved Native Ion-Mobility Mass Spectrometry to Monitor Dynamics of IgG4 Fab Arm Exchange and "Bispecific" Monoclonal Antibody Formation, Anal. Chem. 2013, 85, 9785−9792

[11] P. Olivova, W. Chen, A. B. Chakraborty John C. Gebler, Determination of N-glycosylation sites and site heterogeneity in a monoclonal antibody by electrospray quadrupole ion-mobility time-of-flight mass spectrometry, Rapid Commun. Mass Spectrom. 2008; 22: 29–40

[12] L. F. Pease III, J. T. Elliott, De-Hao Tsai, M. R. Zachariah, M. J. Tarlov, Determination of Protein Aggregation With Differential Mobility Analysis: Application to IgG Antibody, Biotechn. & Bioeng. 101(6), 1214-1222, 2008

[13] K. J. Pacholarz, M. Porrini, R. A. Garlish, R. J. Burnley, R. J. Taylor, A. J. Henry, P. E. Barran, Dynamics of Intact Immunoglobulin G Explored by Drift-Tube Ion- Mobility Mass Spectrometry and Molecular Modeling, Angew. Chem. Int. Ed. 2014, 53, 7765-69

[14] M. Attoui, M. Paragano, J. Cuevas, and J. Fernandez de la Mora, Tandem DMA generation of strictly monomobile 1-3.5 nm particle standards, Aerosol Sci. & Tech., **47(**5), 499-511**,** 2013

[15] J. Rus; D. Moro; J.A. Sillero; J. Royuela, A. Casado, J. Fernández de la Mora, IMS-MS studies based on coupling a Differential Mobility Analyzer (DMA) to commercial API-MS systems, Int. J. Mass Spectrom, **298**, 30-40, 2010.

[16] S. Ude and J. Fernández de la Mora, Molecular monodisperse mobility and mass standards from Electrosprays of tetra-alkyl ammonium halides, J. Aerosol Sci, **36** (10) 1224-1237, 2005.

[17] J. Fernandez de la Mora, High-Resolution Mobility Analysis of Charge-Reduced Electrosprayed Protein Ions, Anal. Chem., 2015, 87, 3729−3735

[18] J. Fernández de la Mora and J. Kozlowski, Hand-held differential mobility analyzers of high resolution for 1-30 nm particles: Design and fabrication considerations. J. Aerosol Sci. (57) 45-53, 2013.

[19] J.L.P. Benesch, B.T. Ruotolo, F. Sobott, J. Wildgoose, A. Gilbert, R. Bateman C.V. Robinson, Quadrupole-Time-of-Flight Mass Spectrometer Modified for Higher-Energy

Dissociation Reduces Protein Assemblies to Peptide Fragments, Anal. Chem., 2009, 81 (3), 1270–1274

[20] C. Larriba-Andaluz and J. Fernandez de la Mora, Gas Phase Structure of Coulombically Stretched Polyethylene Glycol Ions., *J. Phys. Chem. B*, 116, 593-598, 2012

[21] J. Fernandez de la Mora, R. Borrajo-Pelaez, M. Zurita-Gotor Capillary and Coulombic effects on the gas phase structure of electrosprayed Concanavalin A ions and its clusters C_n^{+z} (n=1-6), J. Phys. Chem. B 2012, 116, 9882−9898

[22] You, R.; Li, M.; Guha, S.; Mulholland, G. W.; Zachariah, M. R. Bionanoparticles as Candidate Reference Materials for Mobility Analysis of Nanoparticles Anal. Chem. 2014, 86, 6836−6842

[23] J. Fernández-García, J. Fernández de la Mora, Electrical Mobilities of Multiply-Charged Ionic-Liquid Nanodrops in Air and Carbon Dioxide Over a Wide Temperature Range: Influence of Ion–Induced Dipole Interactions, *Phys. Chem. Chem. Phys.*, 2014, 16 (38), 20500-20513

[24] L. H. Haber, J. Husband, J. Plenge, S. R. Leone, Mobility of t-C4H9 in polar and nonpolar atmospheric gases, Chemical Physics Letters 384 (2004) 219–223

[25] R. Fernández-Maestre, C. S. Harden, R. G. Ewing, C.L. Crawford, H.H. Hill, Chemical standards in ion mobility spectrometry, Analyst, 2010, 135, 1433–1442

[26] N. A. Meyer, K. Root, R. Zenobi, G. Vidal-de-Miguel, Gas-Phase Dopant-Induced Conformational Changes Monitored with Transversal Modulation Ion Mobility Spectrometry, Submitted to Analytical Chemistry, July 2015.

[27] S. Warnke, G. von Helden, K. Pagel, Protein Structure in the Gas Phase: The Influence of Side-Chain Microsolvation, *J. Am. Chem. Soc. 135* (4), 1177-1180, 2013